Band 20 (1984), S. 107—126

ZEITSCHRIFT FÜR
GLETSCHERKUNDE
UND GLAZIALGEOLOGIE


# NUMERICAL EXPERIMENTS ON LARGE-SCALE GLACIAL EROSION

By J. OERLEMANS, Utrecht

With 10 figures

ABSTRACT

Glacial erosion is a very important factor in evolution of landscapes in polar or mountainous regions. Most studies on the large-scale effects of glacial erosion have been of a qualitative nature. Quantitative investigations have been limited to theoretical descriptions of how abrasion depends on factors like basal ice velocity, temperature, debris concentration, normal pressure, and so forth.

In this paper an attempt is made to bridge the gap between qualitative geomorphological ideas and theoretical formulations of the erosion process. To this end a temperature-dependent ice flow model has been developed that includes a description of erosion, lithospheric flexure and flow in the asthenosphere. Numerical experiments are carried out to simulate glacial erosion by valley glaciers as well a by large continental ice sheets. Parameterizations in the model and environmental conditions, such as temperature and mass balance, are varied to study the sensitivity of the results.

The main conclusions are:

(i) For mountain glaciers the evolution of the bedrock profile appears to be determined mainly by climatological conditions. The particular formulation of the 'erosion law' is less important.

(ii) Overdeepening occurs in cases with rather stable termini, i. e. for glaciers ending in the sea or in situations where a slow climatic cooling is present (to counteract retreat associated with lowering of the bedrock due to erosion).

(iii) For polar ice sheets bedrock dynamics allow an exact balance between uplift and erosion rate to be established. However, in the two-dimensional case an instability occurs. A minor valley may develop into a deep glacial trough with higher grounds at its sides due to uplift. This is possible because the transverse scale of the valley is generally smaller than the flexural length scale of the lithosphere.

## NUMERISCHE EXPERIMENTE ZUR GROSSRÄUMIGEN GLAZIALEN EROSION

ZUSAMMENFASSUNG

Glaziale Erosion ist ein wichtiger Faktor für die Entwicklung der Landschaft in Gebirgen und Polargebieten, der im großen Maßstab bisher meist nur qualitativ untersucht worden ist. Quantitative Arbeiten waren auf die theoretische Beschreibung der Zusammenhänge zwischen Abrasion und basaler Fließgeschwindigkeit, Temperatur, Schotterkonzentration, Druck und dergleichen beschränkt.

In der vorliegenden Arbeit wird der Versuch unternommen, die Kluft zwischen qualitativen geomorphologischen Vorstellungen und theoretischen Formulierungen des Erosionsprozesses zu überbrücken. Dazu wurde ein Modell entwickelt, das Erosion, lithosphärische Biegung und

Bewegung in der Asthenosphäre beschreibt. Die Erosion durch Talgletscher und kontinentale Eisschilde wurde numerisch simuliert, wobei die Parametrisierung der mechanischen und klimatischen Bedingungen variiert wurde, um die Sensitivität des Modells zu untersuchen.

Die wichtigsten Ergebnisse sind:

1. Bei Gebirgsgletschern ist die Entwicklung des Untergrundprofils hauptsächlich durch klimatische Größen bestimmt, die Formulierung eines Erosionsgesetzes ist weniger wichtig.
2. Übertiefung tritt bei stationären Zungen auf, also bei Gletschern, die im Meer enden, oder in Situationen, wo langsame Klimaverschlechterung den Gletscherrückzug ausgleicht, der durch die Erosion des Felsuntergrunds hervorgerufen wurde.
3. Bei polaren Eisschilden kann sich ein Gleichgewicht zwischen Hebung des Felsuntergrunds und Erosion einstellen, im zweidimensionalen Modell treten allerdings Instabilitäten auf. Ein kleines Tal kann sich zu einem tiefen Trog entwickeln, dessen Ränder an Höhen gewinnen, weil die Talbreite im allgemeinen kleiner als die charakteristische Länge der Biegung der Lithosphäre ist.

## 1. INTRODUCTION

The variety of landforms and landscapes directly of indirectly due to the erosive action of glaciers is enormous. Wide basins, deep troughs, and a number of smaller scale features such as rock drumlins, cirques, and so forth, occur depending on local conditions and climatic regimes. Many factors are involved in glacial erosion. Sliding velocity, basal ice temperature, basal water production, rock strength and rock permeability all play their role. Also important is the reaction of the earth's crust: ice loading and 'rock unloading' may cause flexure of the lithosphere, with subsequent feedback on the ice flow and erosive action.

A general quantitative theory for the evolution of glacial landscapes is difficult to construct, because so many processes are involved. A wealth of literature on glacial geomorphology exists, and case studies have been made that try to quantify erosion and lodging of particles in terms of glacier properties. Qualitative understanding has been achieved of the many mechanisms seen at work. A fairly complete overview of thoughts and developments in glacial geomorphology was given by Sugden and John (1976). This book also contains an extensive bibliography on the subject. For a discussion on glacial erosion see, for instance, Röthlisberger (1968), Boulton (1974, 1979), Hallet (1981).

Many sites where glacial erosion has occurred have been studied, and classifications according to mechanism, length and time scales involved have been made. Current classifications are, of course, mainly based on direct observations, however, they also suggest the existence of basic physical factors, the precise interaction of which determines the ultimate form of erosion. When looking at features of larger scale, it is tempting to see to what kind of landscapes specific physical laws may lead. For instance, if a bulk erosion rate would be proportional to ice sliding velocity and normal pressure, what would be the profile of a glacial trench after some time? Or, even more specific, would profiles exist for which erosion becomes very small?

Apart from a general geomorphological interest, bedrock erosion also plays an important role in ice-sheet dynamics. Ice flow strongly depends on bedrock profile, and it is conceivable that the general stability of ice sheets depends on how the rock underneath is gradually removed. Concerning the time scales involved in glacial erosion, opinions differ widely. The problem of course is how to infer a bulk erosion rate from a few 'point measurements'. Erosion rates of up to 0.1 or 0.2 m/yr have been

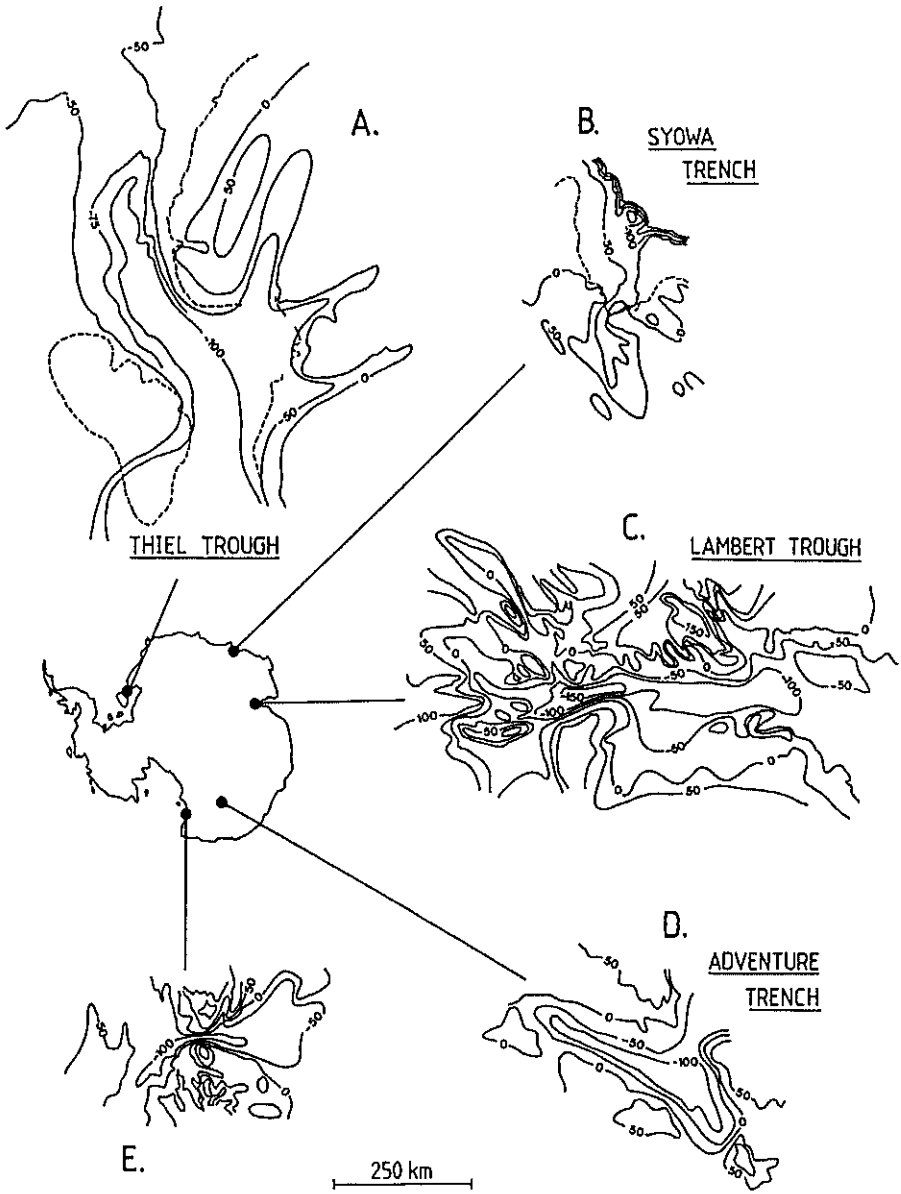


Fig. 1: Some examples of troughs eroded by glaciers. Note the variety in horizontal scale. Contours give bedrock topography relative to sea level, the contour interval is 500 m (numbers on the contours are in decameters). Dashed lines indicate the position of the grounding line (if known). Based on Drewry (1983)

observed at active temperate glaciers (e. g. Vivian 1970), while laboratory experiments on abrasion (Budd et al. 1979) suggest that a few mm/yr is a reasonable figure. Many workers consider one mm/yr to be a characteristic value for more or less 'normal' conditions (e. g. Hallet 1981, Metcalf 1979). This implies that glacial erosion becomes a significant factor in glacier dynamics when the time scale of interest is larger than 50,000 yr, say.

The discussion in this paper is on the global aspects of the feedback between glacier flow, bedrock adjustment (flexure of the lithosphere) and erosion. I will consider large-scale features only, and use models of a highly schematic nature. In many cases the results will probably not be of direct value to the field glaciologist. However, they may help to set the stage for a more unified approach, in which the feedback mentioned above is just a component of the global climate system.

Introductory considerations should specify the space and time scales of interest. As a start, consider a number of bedrock features observed in Antarctica, which are probably all related to some extent to the action of glacial erosion. Fig. 1 shows maps of bedrock topography in several areas (redrawn from Drewry, 1983). The Thiel Trough is an example of a trough with large spatial scale. It is presently covered by the Filchner Ice Shelf, with Berkner Island (grounded ice) in the lower-left part of the figure. The Thiel Trough was probably formed during times in which grounded ice extended over the Weddell Sea. The lateral and longitudinal length scales of Thiel Trough are about 200 and 1000 km, respectively.

The Syowa Trench (B) is a smaller scale disturbance. It is about 500 m deep, and has a width of only a few tens of kilometers at the grounding line. The trench accomodates an active glacier and can be considered as a 'young trough in development'. There are about ten to fifteen of these small-scale coastal troughs in East Antarctica.

The trough through which Lambert Glacier flows to feed the Amery Shelf is the most impressive feature in East Antarctica (C). It is over 1500 m deep with many side troughs (see also Morgan and Budd 1975). A large part of the ice mass accumulated over East Antarctica flows through this trough. Maybe Lambert Trough started as a small trench like the Syowa Trench. On the seaward side the lateral scale is 100 km or more, but in the deepest central part it may be 50 km. A reasonable value for the longitudinal scale is 1000 km.

Adventure Trench (D) is not located on the coast. It is a subglacial trench about 1000 m deep and could be due to erosion. The lateral scale is about 100 to 200 km.

Many troughs of small scale can be found in the Transantarctic Mountains; an example is shown in E. These troughs are narrow, and are similar to the troughs found in Greenland, Norway and other places. The lateral scale is typically 5 to 50 km.

These examples reveal that typical transverse length scales are in the 10 to 300 km range, while longitudinal length scales are substantially larger: 500 to 1000 km, say. This observation is important for the discussion in the next section, where the basic physical factors are investigated.

## 2. BASIC CONSIDERATIONS

Before describing a numerical model of the ice flow / lithospheric flexure / erosion interaction, we first study more qualitatively which factors are important under different conditions.

Concerning the process of glacial erosion, distinction is normally made between

abrasion and plucking (e. g. Sugden and John 1976). We will ignore this distinction, and work with a bulk erosion rate E. The effect of all processes leading to removal of rock is supposed to be included in E. Two factors are supposed to be of primary importance: ice sliding velocity and normal load (including the effect of basal water pressure). Boulton (1974), among others, considers ice thickness as a controlling variable. Here this will not be done, because the link between rate of erosion (or deposition) and ice thickness probably operates via other quantities like basal ice temperature and normal pressure. In this study we only consider a functional relationship of the type $E(V_s, N)$, in which $V_s$ is the sliding velocity and N the effective normal pressure (ice load minus basal water pressure). Note that, since in many parameterizations of basal sliding $V_s$ is expressed in terms of normal pressure and basal shear stress $\tau$, E can also be expressed in $\tau$ and N, or in $\tau$ and $V_s$. Laboratory work by Budd et al. (1979), for instance, suggests that

$$E = \mu \tau N V_s^{1/3}, \tag{1}$$

where $\mu$ is a constant depending on the type of material. Here $\tau$ can be eliminated once a flow law for sliding has been adopted.

Although ice temperature does not explicitly occur in Eq. (1), it enters the problem in many ways. Significant sliding only occurs when basal ice is temperate, and meltwater that is not removed in an efficient way will reduce the normal pressure. It thus turns out to be necessary to calculate the temperature field in the glacier or ice sheet, unless one can be sure that basal ice is at pressure melting everywhere. In this paper we will also consider cold ice sheets and glaciers, so the temperature computation is included in all cases.

The role of lithospheric flexure depends very much on the spatial scale of the variations in loading. Deflection of the lithosphere due to a line load may illustrate this. Supposing that the lithospere can be considered as a thin elastic shell, the balance of forces reads (see, for example, Turcotte 1979):

$$D \frac{d^4 S}{dx^4} + \rho_m g S = q, \tag{2}$$

where D is flexural rigidity, S deflection, $\rho_m$ characteristic mantle rock density, g gravitational acceleration and q the applied load. This equation has the solution

$$S(x) = \frac{q \alpha^3}{8 D} e^{-x'} [\cos x' + \sin x'] \tag{3}$$

$$\text{where } x' = |x|/\alpha, \ \alpha = [4 D / g \rho_m]^{1/4}.$$

This solution is plotted in fig. 2. The quantity $\alpha$ can be considered to be a typical length scale for the response of the lithosphere to a load. Since the continental lithosphere is generally thicker than the oceanic lithosphere, it has a larger effective rigidity. Thus a reasonable value of $\alpha$ for present purposes is 150 km (Turcotte and Schubert 1982).

We now distinguish between three typical cases, based on the characteristic length L of the load. When $\alpha \ll L$, local isostatic equilibrium will always be established. Erosive features cannot develop, because removal of rock will locally be compensated by uplift. When $L \ll \alpha$, the lithosphere is essentially rigid. Formation of a glacial trough will lead to general uplift of a larger area, while the shape of the trough-mountain system is hardly affected.

In the third case we have $L \sim \alpha$, and substantial interaction between erosion, ice

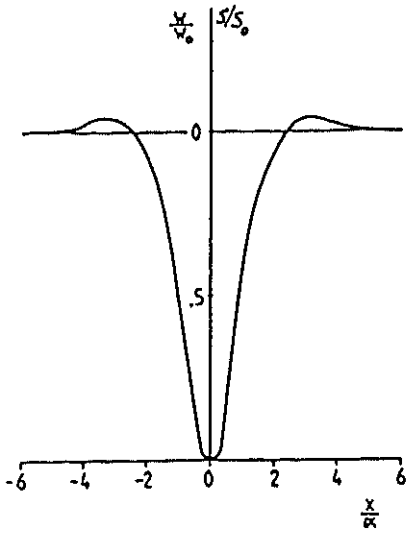


Fig. 2: Nondimensional flexure of the lithosphere under a line load. The flexural length scale (order of magnitude: 100 km) is denoted by $\alpha$

flow and crustal flexure has to be expected. When looking back at fig. 1, it turns out that in many cases $L \sim \alpha$. However, for narrow troughs accomodating valley glaciers, lithospheric flexure may be neglected.

When the bedrock topography changes, the ice flow will react. Since over polar ice sheets accumulation is generally small, it may take a long time before the ice flow reaches a new balance. In such cases it may be necessary to calculate the response of the bedrock explicitly, that is, all relevant equations have to be integrated simultaneously because there is no clear separation in the time scales.

Based on the forgoing considerations it will be obvious that a global study of glacial erosion requires a model that carries ice flow, ice temperature, erosion rate and bedrock elevation as space and time-dependent variables. This list is a minimum. In a later stage of model development, factors like debris content of basal ice and its effect on sliding and erosion, and glacial hydrology should be taken into account.

## 3. DESCRIPTION OF THE MODEL

A simple ice-sheet model is used, in which the vertical mean ice velocity is directly related to the driving stress and, for the sliding component, to the effective normal pressure. The local rate of change of ice thickness H is calculated from the vertically-integrated continuity equation. Since ice density is assumed to be constant, we have:

$$\frac{\partial H}{\partial t} = -\nabla \cdot H U + M. \tag{4}$$

U is the vertical mean ice velocity parallel to the bedrock and M the annual ice accumulation rate, see fig. 3. Mass convergence due to curvature of the bedrock is neglected. M will be specified later; depending on the specific purpose it may be a func-

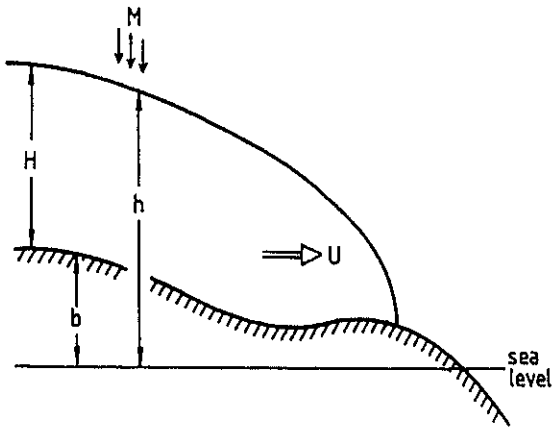


Fig. 3: Geometry of the model ice sheet

tion of elevation and/or slope, distance to moisture source, and so forth. The $\nabla$-operator is understood to be two-dimensional (parallel to the bed).

The ice velocity U is split into two contributions: one from internal deformation ($U_d$) and one from basal sliding ($U_s$). We assume that $U_d$ depends on basal ice temperature $\theta_0$ and basal stress $\tau$, because of the velocity shear takes place in the lower layers (e. g. Paterson 1981). $U_s$ is expressed in ice temperature, basal stress and normal pressure N (Budd et al. 1979). The flow laws used are:

$$
\begin{aligned}
U_{dx} &= F_1 H \tau_*^{n-1} t_{xz} \\
U_{dy} &= F_1 H \tau_*^{n-1} \tau_{yz} \\
U_{sx} &= F_2 \tau_*^{n-1} \tau_{xz}/N \\
U_{sy} &= F_2 \tau_*^{n-1} \tau_{yz}/N
\end{aligned} \tag{5}
$$

The x,y-plane is parallel to the local bed. Normal stress deviators are neglected, so the basal stress is set equal to the driving stress defined below. The effective stress $\tau_*$ is:

$$\tau_* = [\tau_{xz}^2 + \tau_{yz}^2]^{1/2}. \tag{6}$$

The flow parameters $F_1$ and $F_2$ depend on ice temperature. The normal pressure N is the weight of the ice column minus the subglacial water pressure. The large-scale driving stress can be approximated by (h is surface elevation):

$$
\begin{aligned}
\tau_{xz} &= -\rho g H \frac{\partial h}{\partial x} \\
\tau_{yz} &= -\rho g H \frac{\partial h}{\partial y}
\end{aligned} \tag{7}
$$

Inserting this in eq. (5), and assuming that $n=3$, we find

$$U_{dx} = -F_1 (\rho g)^3 H^4 \left[ \left( \frac{\partial h}{\partial x} \right)^2 + \left( \frac{\partial h}{\partial y} \right)^2 \right] \frac{\partial h}{\partial x}, \tag{8}$$

and similar expressions for the other velocity components. After some algebraic manipulations it turns out that eqs. (4), (5), (6) and (7) can be combined to give a single equation for the evolution of ice thickness. It reads

$$\frac{\partial H}{\partial t} = \nabla \cdot D_i \nabla h + M \tag{9}$$

$$D_i = (\rho g H)^3 \left[ \left( \frac{\partial h}{\partial x} \right)^2 + \left( \frac{\partial g}{\partial y} \right)^2 \right] (F_1 H + F_2 / N) \cdot H \tag{10}$$

Eq. (9) is in fact a nonlinear diffusion equation, in which the 'diffusivity for ice mass' $D_i$ increases strongly with ice thickness and surface slope, and decreases with normal pressure (apart from temperature effects).

As noted earlier, $F_1$ is a function of basal ice temperature only, because most of the shear strain occurs in the lower layers. $F_2$ should describe the transition from an essentially non-sliding regime to a sliding regime. Opinions on how to formulate this differ widely (for a review, see Lliboutry, 1979). Here hydraulics of subglacial water also come into play (e. g. Bindschadler 1983), but at present it is difficult to find a satisfactory treatment for global models. We will not use a step function of $F_2$, but let it depend in a smooth way on basal temperature. In the present model, the transition from a sliding to a non-sliding regime is gradual for two reasons. Firstly, each grid point represents average conditions over a large area, through which there are temperature fluctuations anywhere. So a somewhat smoothed flow law is preferable. Secondly, a very steep dependence of $F_2$ on basal temperature would put heavy demands on the numerical scheme. Some tests were done to investigate this point. Although it turned out that numerical stability could always be achieved, the time step required was so small (fraction of a year for valley glaciers) that efficient integrations could not be done.

The flow parameters actually used in this study are:

$$F_1 = 3.2 \times 10^{-23} \exp[0.23\,(\theta_0 - T_m)]\ \mathrm{m^6 s^{-1} N^{-3}}$$

$$F_2 = 6.4 \times 10^{-16} \exp[\theta_0 - T_m]\ \mathrm{m^5 s^{-1} N^{-2}}$$

In these expressions $T_m$ is the pressure melting point. The value of $F_2$ in case of melting at the base is close to the one found by Bindschadler (1983). The value for $F_1$ is rather ambiguous, because different sources give different numbers (for a discussion, see for instance Paterson 1981).

Calculation of ice temperature $\theta$ is based on the thermodynamic equation:

$$\frac{\partial \theta}{\partial t} = k \nabla^2 \theta - \bar{v} \cdot \nabla \theta + \Phi \tag{11}$$

Here k is thermal diffusivity, $\bar{v}$ three-dimensional ice velocity and $\Phi$ frictional heating. An approximating method is used to solve eq. (11). Firstly, horizontal diffusion is neglected, so the diffusion therm reduces to $k \partial^2 \theta / \partial z^2$. Next, the temperature field is expanded in powers of z, the height above bedrock. So

$$\theta(x, y, z, t) = \theta_0(x, y, t) + z\theta(x, y, t) + z^2 \theta_2(x, y, t) + \ldots \tag{12}$$

Three terms in the expansion are retained. Equations for $\theta_0$, $\theta_1$ and $\theta_2$ are obtained from:

(i) the lower boundary condition ($\partial \theta / \partial z$ matches the prescribed geothermal heat flux);

(ii) the upper boundary condition ($\theta_s = \theta_0 + \theta_1 H + \theta_2 H^2$ equals the annual surface temperature);

(iii) the vertically-integrated form of eq. (11).

Here we will not treat the details of the procedure, but only mention some aspects. The method of solving the thermodynamic equation is fully described in Oerlemans (1982).

The integration of eq. (11) over the depth of the ice sheet requires a specification of the velocity field. In the present study, the velocity profile due to deformation is assumed to be parabolic in z, scaled in such a way that velocity averaged over depth equals the one given in eq. (5). Such an approximation seems to be compatible with the representation of the vertical temperature profile. The vertical velocity (relative to the bedrock, i. e. dz/dt) then follows from the three-dimensional continuity equation together with the upper boundary condition:

$$w_h = \frac{\partial H}{\partial t} + u_h \frac{\partial H}{\partial x} - M. \tag{13}$$

Frictional heating is calculated from the release of gravitational energy by downward motion. This is possible because the kinetic energy of the ice flow is extremely small. Note that in the calculation of frictional heating the absolute velocity should be used, not dz/dt as defined above! In the model, frictional heating by slip is released at the base of the ice sheet, while deformational heating is partitioned: one part (50 % in the experiments discussed here) is also added to the base, the remaining part comes to the vertical mean heat budget and thus increases the vertical mean temperature.

We finally consider the bedrock dynamics. The representation of the crust consists of an elastic shell (representing the lithosphere) resting on a viscous asthenosphere. The rigidity of the lithosphere, denoted by D, determines the ultimate response to loading. The governing equation is:

$$D \nabla^4 S + \rho_m g S = g(\rho H - \rho_m E_t). \tag{14}$$

Here S is the deflection (positive downwards), $\rho_m$ mantle rock density, $E_t$ total amount of removed rock. Eq. (14) is linear, and is most conveniently solved by a Fourier-transform method. Since this is a standard procedure, the method will not be discussed here.

Whereas the rigidity of the lithosphere determines the ultimate equilibrium deflection pattern, the viscous flow in the asthenosphere governs the time scale on which the adjustment takes place. With the usual assumptions, such as that deflection is much smaller than the effective depth of the asthenosphere, the equation describing the vertical bedrock displacement turns out to be (Oerlemans and Van der Veen 1984):

$$\frac{\partial Z_b}{\partial t} = D_b \nabla^2 [Z_{b0} - Z_b + S]. \tag{15}$$

In this equation $Z_b$ is the depression relative to the undisturbed value $Z_{b0}$. So again we encounter a diffusion equation. The coefficient $D_b$ is inversely proportional to the mean viscosity of the asthenosphere and proportional to the third power of the effective depth of the asthenosphere. The real bed elevation now follows from:

$$b = b_0 - E_t - Z_b, \qquad \text{while } h = b + H. \tag{16}$$

This concludes the basic formulation of the model. The set of equations discussed above is integrated numerically on a grid. Forward time differencing is used for all equations, with a Lax-Wendroff correction method (e. g. Mesinger and Arakawa 1976) for the advection terms in the heat equation. A staggered grid in space is used to solve the nonlinear diffusion equation governing changes in ice thickness.

## 4. EXPERIMENTS ON VALLEY GLACIERS

Valley glaciers have the convenient property that they follow orographic features. In a plan view, a flow line can be interpreted as a trajectory, even when the glacier is not in equilibrium. Glaciers can therefore be simulated to some extent by one-dimensional models. The numerical experiments discussed in this section were all carried out on a one-dimensional grid with 31 grid points, spaced at 2.5 km.

To obtain realistic glacier profiles, a varying width of the glacier basin should be included. For the schematic experiments discussed here the glacier's width is prescribed as

$$B = B_0 e^{-x/L^*}. \tag{17}$$

$L^*$ thus represents a typical length over which the glacier width drops to 1/e of its value high up in the accumulation area, say.

The appropriate continuity equation now becomes

$$\frac{\partial H}{\partial t} = -\frac{\partial}{\partial x}(H U) - \frac{U H}{B}\frac{\partial B}{\partial x} + M, \tag{18}$$

where H, U and M are now representing mean values over the width of the glacier. So the relevant factor concerning the geometry is $(\partial B/\partial x)/B$, and according to eq. 17) this factor equals $-1/L^*$.

Mass-balance conditions are formulated as follows:

$$M = \min\,[(h - h_E)\,C_1;\, C_2], \tag{19}$$

where $h_E$ is the equilibrium-line elevation, $C_1$ the mass-balance gradient and $C_2$ the upper limit in the accumulation zone. In addition to this the surface temperature has to be specified. Observations in the Alps suggest that firn temperature remains close to the melting point as long as the annual air temperature does not drop below about $-8°$ C (e. g. Haeberli 1983). In the present experiments on valley glaciers, surface temperature is therefore prescribed as

$$\theta_s = \min\,[T_E + 8 + \gamma(h - h_E);\, 0]\ °\mathrm{C}. \tag{20}$$

$T_E$ is the annual air temperature at the equilibrium line and $\gamma$ the lapse rate (set to $-7°$ C/km). Eq. (20) is admittedly a rather crude parameterization of the surface temperature along the glacier, but probably serves the present purpose.

As reviewed by Haeberli (1983), mass-balance gradient, maximum accumulation rate and temperature at the equilibrium line are related. We therefore select a few typical cases. In the first experiment we consider a large maritime glacier, with $C_1 = 0.01\ \mathrm{yr}^{-1}$, $C_2 = 2$ m/yr and $T_E = -2°$ C. All values referring to mass balance are in m ice depth. Eq. (1) was used to calculated the bulk erosion rate, i. e. following Budd et al. (1979). With constant effective normal pressure (grade line 50 m below the ice surface), this implies that the rate of erosion is proportional to the base stress, and to the sliding velocity to power 1/3. The geothermal heat flux, which is of minor importance anyway, was set to 0.05 W/m$^2$.

The result is shown in fig. 4a. In this integration the snow line is at 1800 m. A 70 km long glacier is then established within 1000 yr of simulated time, and basal ice is at the melting point everywhere. Sliding and deformation are about equally important. The erosion rate is fairly constant, with a weak maximum in the vicinity of the equilibrium line due to high ice velocities. The gradual lowering of the bedrock has a strong

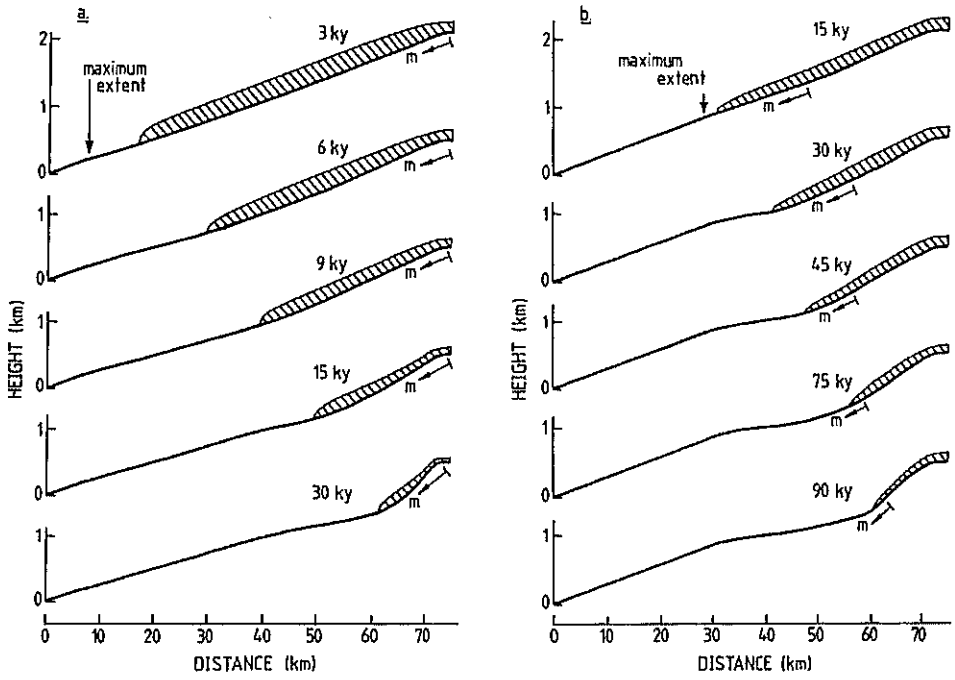


Fig. 4: Evolution of the bedrock-glacier system, in case of a warm maritime glacier (a) and a cold continental glacier (b). The elevation of the equilibrium line is 1800 m in both cases. Arrows at the base indicate basal melting

impact on the length of the glacier. The mass-balance gradient is large, and, since the accumulation is more or less constant, a lowering of the bedrock in the ablation zone must lead to substantial retreat. After 30 ky the glacier volume is reduced to a fraction of the volume at 3 ky. However, time scales are highly uncertain, of course. At this point it is important to note that the results do not really depend on the erosion constant $\mu$ as long as the time scale for erosion is substantially larger than that for the glacier dynamics. So halving $\mu$ leads to approximately the same bed profiles when simulated time in fig. 4 is doubled.

This experiment was repeated with the erosion rate proportional to sliding velocity only. The result was very similar, which is not surprising because stress and sliding velocity are closely related in the parameterizations employed in the present model. In another run the grade line was set to one quarter of the ice thickness below the surface of the glacier, just to test the sensitivity to the distribution of normal pressure. Again, differences with the first experiment were very small (differences in bed profiles less than 20 m).

In a second experiment, cold continental conditions were applied: $C_1 = 0.003\ \mathrm{yr}^{-1}$, $C_2 = 0.5$ m/yr and $T_E = -14°$ C. The equilibrium line was again at 1800 m. Fig. 4b shows the results. In spite of the fact that the glacier is cold now over the upper two thirds, its thickness is much less than in the 'maritime case'. Here, the much smaller mass-balance gradient is the dominating factor. As expected, the glacier-bed system

evolves at a much slower rate, with a stronger tendency to form a terrace-type bed profile. The sensitivity of this solution to changes in the formulation of the erosion rate was tested in a similar way as for the first experiment. Again, the sensitivity turned out to be rather small.

In order to find out how important the climatic environment of the glacier is, numerical integrations were carried out for specific 'climatic scenarios' in which the movement of the equilibrium line is prescribed. As already anticipated from the previous results, minor changes in the height of the equilibrium line can have a strong impact on the particular evolution of the bed profile. An example is shown in fig. 5.

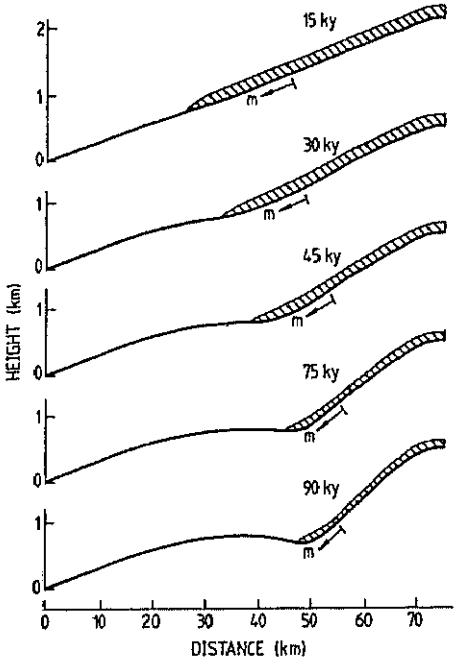


Fig. 5: As in fig. 4b, but with an additional lowering of the equilibrium line by 4 m per 1000 yr

The experiment is completely similar to the one displayed in fig. 4b, except that now the equilibrium line descends at a rate of 4 m in thousand years. This apparently creates conditions very favourable for the formation of overdeepenings, because the warm-based snout of the glacier can stay in roughly the same position for a long time.

The results of the numerical experiments on alpine glaciers can be summarized in two points:

(i) The bedrock profile that evolves is rather insensitive to the particular 'erosion law' used. The reason is that the glacier withdraws when the bed has reached some specific elevation. This tends to create rather flat valleys with a steep slope at the end. So the climatological conditions determine to a large extent the evolution of the bed profile.

(ii) The occurrence of overdeepenings is favoured by a gradually deteriorating climate, or slow uplift of the entire region. Large catchments also help, because glacier retreat due to a lowering bed is less in such cases.

Of course, many questions can be raised, for instance: What would happen when the equilibrium line moves up and down in a short time, or when it moves periodically.

What is the effect of varying valley width?, and so forth. Such questions are interesting and will certainly be investigated in further work. However, they are outside the scope of the present paper, because its intention is to show the possibilities of dynamic modelling of the glacier-bedrock system, not to carry out case studies.

To conclude this section we finally consider an experiment on a glacier in very cold climatic conditions. The glacier will then have its terminus at the coast, and retreat is expected to be less when the bedrock lowers due to erosion. The experiment was performed on a 5 km grid, with erosion rate proportional to sliding velocity. For the initial bedrock profile, see fig. 6. The equilibrium line was prescribed to sink linearly in time, until it reached an elevation of 300 above sea level (at t=20 ky). Other model constants used: $C_1 = 0.003\ yr^{-1}$, $C_2 = 1$ m/yr, $T_E = -10°$ C.

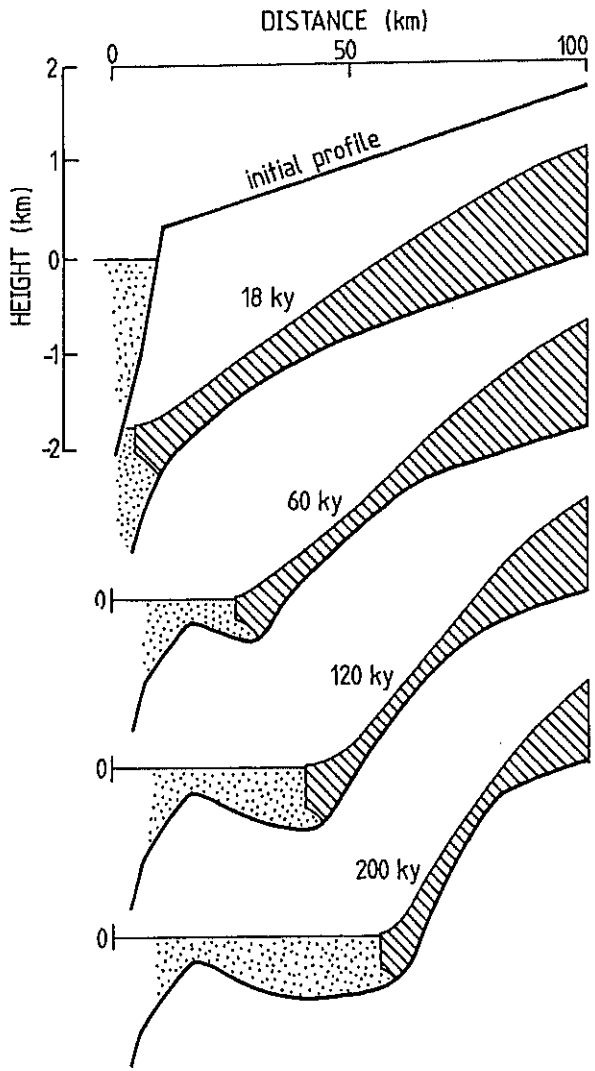


Fig. 6: An example of glacier erosion in a cold climate. The equilibrium line sinks linearly in time, and after 20 ky is kept fixed at 300 m above sea level

When a model glacier ends in the sea, ice-shelf dynamics should be included. In fact the complete grounding line problem, a major problem in glaciology, is encountered. Here only a schematic treatment is employed, with a flotation condition and a prescribed profile of the ice shelf to determine the position of the grounding line. For the present type of experiments this should be sufficiently accurate.

As shown in fig. 6, retreat of the glacier is steady, and it leaves behind a submarine valley with significant overdeepening (about 450 m). After 200 ky of simulated time, the bedrock underneath the glacier becomes so steep that the numerical scheeme breaks down (the truncation error in the heat advection terms becomes too large). Further integration would be possible by using smaller and smaller time steps, but the basic feature is already clear. This pilot experiment in fact suggests that large overdeepening should be expected in cold climates, in which glaciers are not so sensitive to variations in the height of the equilibrium line as in alpine climates with high temperatures in the valleys. This, by the way, is in accordance with observations: overdeepened fjords occur in Norway, Baffin Island, Greenland and Antarctica (fig. 1).

## 5. POLAR ICE SHEETS: FLOW-LINE EXPERIMENTS

In this section we consider calculations more relevant to the dynamics of large ice sheets. We turn to a larger space scale, but still use a one-dimensional model. All horizontal derivatives perpendicular to the flow line are assumed to be zero, and a much coarser grid is used (40 km grid-point spacing). Further modifications involve reformulation of the mass balance equation and inclusion of bedrock dynamics as described in section 3.

From the climatology of the Antarctic Ice Sheet it is known that accumulation is generally largest at the ice-sheet edge and drops off rapidly with surface elevation (e. g. Atlas Antarktiki 1966). Typical conditons are represented by:

$$M = 0.5 \exp(-h/1500) \quad \text{m/yr}, \tag{21}$$

where h is in meters. Characteristic values of annual sea-level temperature and lapse rate are $-15°$ C and $0.01°$ C/m.

Because of the large scale involved, the movement of the bedrock now has to be calculated (in the one-dimensional fashion). Model parameters used for the bedrock dynamics are: $D = 8.5 \times 10^{24}$ N m and $D_b = 1.58$ m$^2$/yr. For a discussion of such parameter values, see Walcott (1970), Turcotte and Schubert (1982). The initial bedrock profile prior to developing an ice cover consists of 4 grid points at $-3000$ m, next to the steep continental edge, and then the continent with zero surface elevation. The four 'deep' grid points are required to avoid spurious effects of the boundary conditions on the solutions. The initial profile is shown by the dashed line in fig. 7.

In the first experiment the annual sea-level temperature was set to $-18°$ C. Starting from no ice cover, an ice sheet builds up and gradually depresses the bedrock. After some time, which depends on the erosion constant $\mu$, but is typically a few hundred ky, a stable equilibrium state appears to be reached. This state is shown in fig. 7. The mean ice thickness is a few kilometers, and the basal ice temperature is at the melting point in the thicker half of the ice sheet. The zone of low basal temperatures near the edge is due to the much higher accumulation there, see eq. (21). Since an equilibrium exists, the erosion rate equals the uplift everywhere. The dependence of ero-

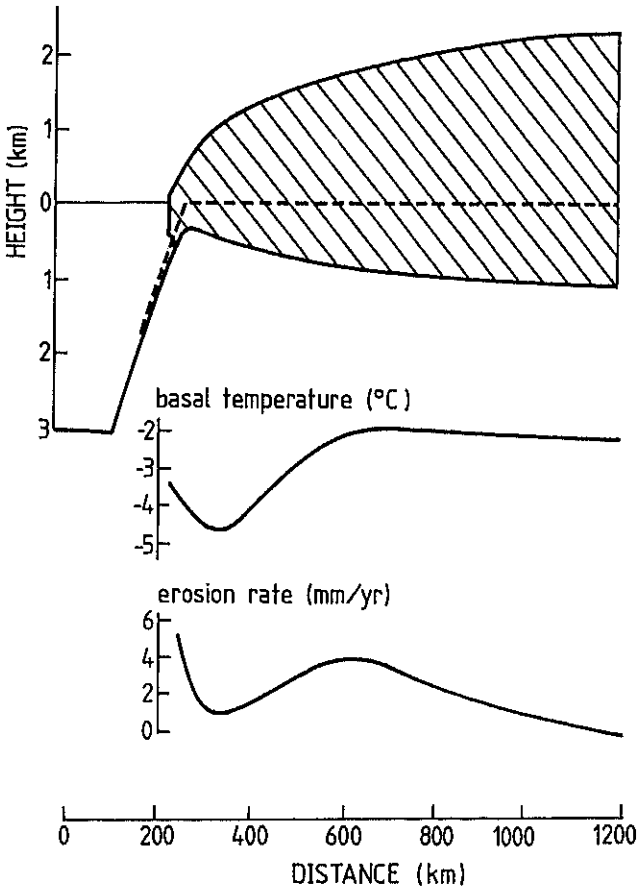


Fig. 7: Simulation of a polar ice sheet, with calculation of lithospheric flexure. The initial profile is a flat continent bounded by deep ocean. A study state is ultimately reached, in which uplift exactly compensates erosion. See text for model parameters

sion rate on basal temperature is clearly seen. The large erosion rate near the edge is a consequence of the high sliding velocity.

Fig. 8 shows the result of a similar experiment, but now with the annual sea-level temperature set to $-12°$ C. Apparently, this strongly effects the rate of erosion, which now increases monotonically towards the ice-sheet edge. The shape of the ice sheet, however, is not very much different from that in fig. 7. The uplift mechanism apparently acts as a buffer, compensating for variations in erosion.

The stable behaviour of this ice sheet-bedrock system finds its origin in the damping associated with variations in ice thickness and ice velocity. For example, if for some reason the erosion rate decreases at a particular point, the ice will become thinner compared to the surroundings. Because of mass-balance requirements, this causes an increased ice velocity and consequently an increased rate of erosion. In this way, small-scale perturbations in the bedrock profile are quickly damped (note that in all experiments discussed so far the strength of the bedrock is constant!).

To illustrate the strong effect of lithospheric bending, one run was carried out with all parameter values as in the previously discussed experiment, except that movement

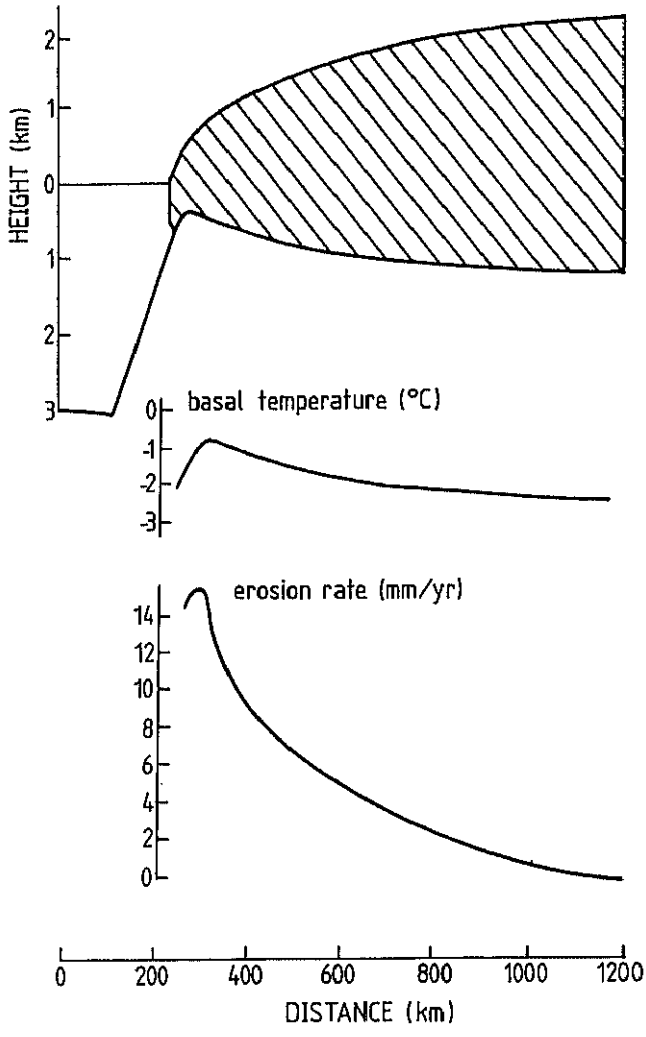


Fig. 8: Same as fig. 7, except for a change in surface temperature of +6° C. Although the erosion pattern is quite different, the bed profile and shape of the ice sheet have hardly changed

of the bedrock was not allowed. A few profiles are shown in fig. 9. As expected, the model ice sheet steadily retreats in this case. In fact, the result is rather similar to that shown in fig. 6. Although in reality the lithosphere will bend when conditions in the transverse direction are homogeneous, this experiment has some relevance. For example, if this flow line represented an ice stream with a width smaller than the flexural length scale, with relatively stagnant ice at its sides, transverse forces would not permit bending. It is then possible that the grounding line of the ice stream would retreat over long distances as a consequence of glacial erosion.

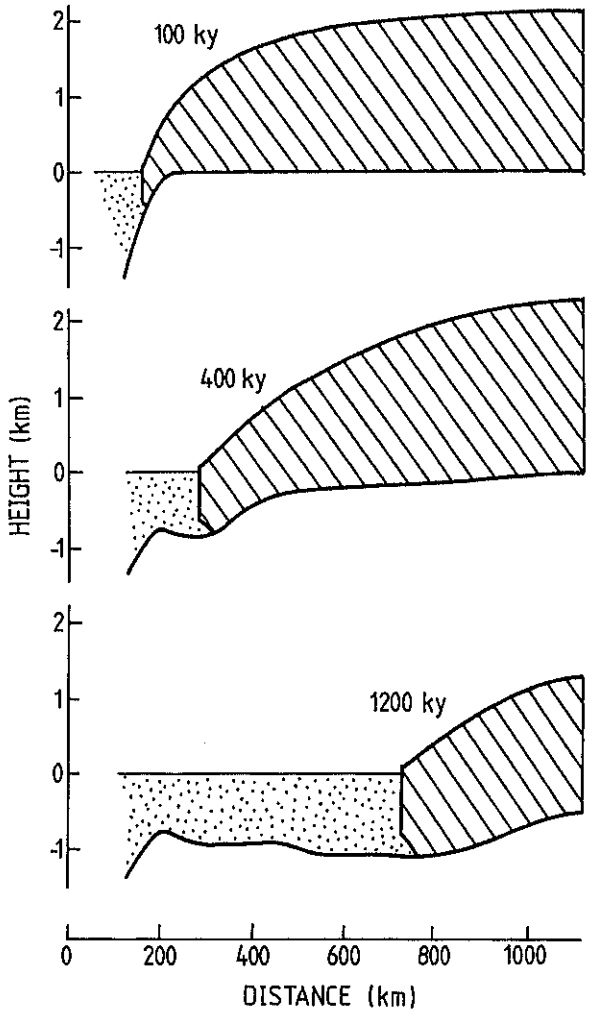


Fig. 9: This run shows what happens if lithospheric bending is not taken into account. All model parameters are the same as for the experiment shown in fig. 8

## 6. POLAR ICE SHEETS: A TWO-DIMENSIONAL EXPERIMENT

Two-dimensional experiments consume much more computer time, of course, but also allow a better simulation in cases where erosive features have dimensions comparable to the flexural length scale of the lithosphere. The few experiments described in this section are meant to illustrate this point.

Integrations are now carried out on a 21 by 21 grid, with points spaced at 20 km. This is admittedly not a very high resolution, but it is necessary to keep processor times within reasonable bounds. In the initial state the continental bed is flat with an elevation of 200 m above sea level. At one side, this piece of continent is bounded by deep ocean, at the other sides conditions are symmetric, so there is no flow of ice into

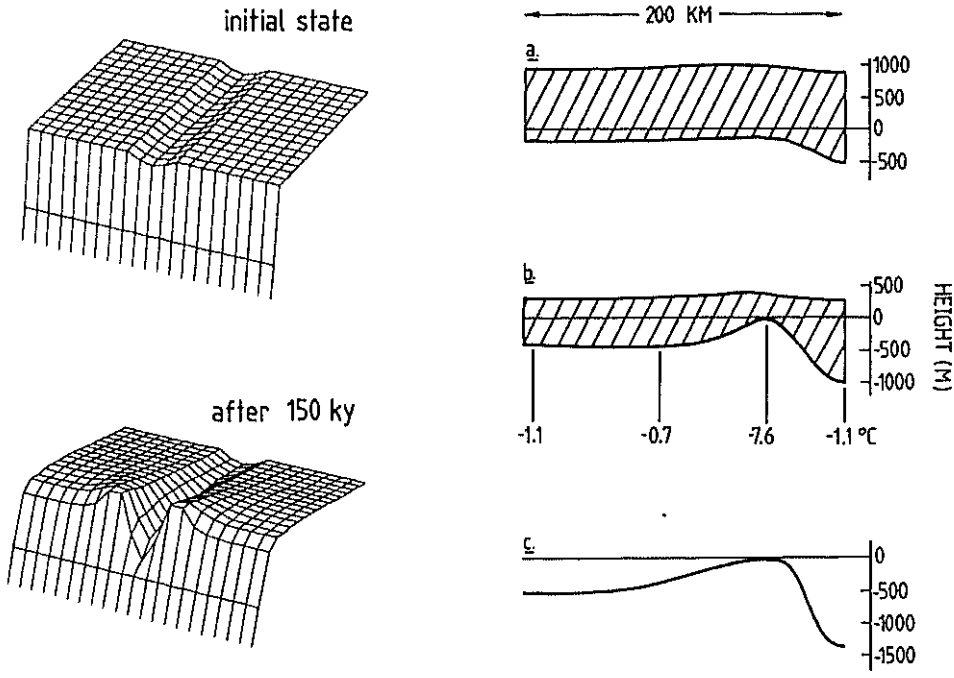


Fig. 10: Some results from a two-dimensional experiment. The left-hand side shows isometric plots of initial bedrock topography and the trough as formed after 150 ky of simulated time. The right-hand side shows some cross sections parallel to the coast line. Section a is about 110 km from the grounding line, section b about 10 km. For the last section some basal temperatures are indicated. The profile shown under c is an experiment with erosion rate proportional to sliding velocity only

or out of these sides. Furthermore, a valley 60 km wide and 150 m deep, running from the ice divide to the ocean, is added to the topography. The purpose of the experiment now is to see how this minor valley develops during glacierization. Model constants used are the same as given in section 5. In the first run, Budd's relation for the erosion rate was used again. Sea-level temperature was set to $-16°$ C, with the mass-balance formulation according to eq. (21).

Results are summarized in fig. 10. The left-hand side shows the bedrock topography after 150 ky of simulated time. The three cross sections at the right-hand side are parallel to the coastline. Close to the coast the valley has deepened substantially, and bedrock has been uplifted at its sides. The strength of the lithosphere thus allows a trough to form. Large-scale uplift associated with the erosion in the trough causes the high areas to occur. No equilibrium is reached, as will be clear when looking at the basal temperatures. In the trough basal ice is at the melting point, whereas on the ridge basal temperature is low. Consequently, ice velocity and erosion rates are large in the trough, and small on the ridges. Substantial erosion also occurs closer to the lateral boundaries of the model. Here the situation is somewhat like that depicted in fig. 7.

The integration was carried out a little bit further than shown in fig. 10. This led to

steepening of the sides of the trough until truncation errors in the numerical scheme became so large that instability occurred.

A second experiment was conducted with erosion rate proportional to sliding velocity only. This appeared to have amazingly little effect (again) on the evolution of the bed topography. The cross sectional profile close to the coastline, in a stage comparable to the results of the previous run, is shown at the bottom of fig. 10.

The most important conclusion to be drawn from these experiments is that minor irregularities, like small valleys, may develop into trough-like features with large ice discharge (velocities up to hundreds of meters per year), surrounded by cold stagnant ice (velocities of only a few meters per year) on higher bedrock. Such configurations are frequently encountered on East Antarctica, where climatological conditions are similar to those used in the model experiments. Perhaps Lambert Glacier Trough can be seen as a nice example of instability of the ice sheet-bedrock system, in which the rigidity of the lithosphere enables the ice flow to penetrate deeper and deeper.

In the few experiments discussed above, the grounding line did not retreat in the trough. Apparently, the large discharge of ice into the trough prevents this from happening. Here grounding line dynamics come into play again, and it is unlikely that the present approach is sufficiently accurate to determine whether grounding-line retreat occurs or not.

## 7. FINAL REMARKS

The experiments discussed are of a schematic nature. This may be seen as a serious drawback, but on the other hand it makes an integrated approach possible, in which a general model of the ice sheet-bedrock system can be applied to landforms with various spatial scales. So far, quantitative studies of glacial erosion have been local, and studies of how glacial landscapes evolve have been qualitative. This paper makes a start at bridging this gap.

This paper is also meant to set the stage for more detailed studies. Case studies of observed eroded bedrock profiles should make it possible to narrow down the range of values of empirical parameters in 'erosion laws'. It is not unthinkable that observed bedrock profiles tell more about how, on the large scale, sliding and erosion ultimately work than local measurements do. When the climatic history is fairly well known, such studies seem promising.

Another point of great importance is whether erosion destabilizes continental ice sheets. The stability of West Antarctica, for example, cannot be studied without considering the effect of glacial erosion on the ice flow. On time scales of tens of thousands of years, glacial erosion can be just as important in grounding-line migration as variations in sea level are. Even the development of ice streams and stagnant ice zones may be linked to the erosion — ice velocity coupling in a yet unclear way.

Lodging of particles has not been considered in this paper. In all experiments described here the assumption was made that debris is completely removed. This point will also be taken up in future work. It has been stressed by Hallet (1981) that both sliding velocity and abrasion depend on the debris concentration of the basal ice. In principle, such effects can be taken into account by adding to the model an equation that describes the debris concentration. Parameterization of subglacial lodging will be particularly difficult. It is yet not clear, however, that this process is really important in the formation of large-scale features like glacial troughs.

Finally, it should be noted that basal water pressure was treated in a simple way. The water table was prescribed to be a fixed distance below the ice surface, which is a reasonable approach in view of the insensitivity of the results to the particular erosion law used. Nevertheless, a more accurate approach should be possible, for instance along the lines discussed by Bindschadler (1983), based on Röhtlisberger's (1972) theory.

ACKNOWLEDGEMENT

Although I did not follow all the suggestions, this paper certainly benefitted from comments by C. J. van der Veen, C. J. E. Schuurmans, B. Hallet and R. Hooke.

REFERENCES

Atlas Antarktiki, 1966: Glavnoje Upravlenie Geodezii i Kartografii MG, Moskva - Leningrad.

Bindschadler, R., 1983: The importance of pressurized subglacial water in separation and sliding at the glacier bed. J. Glaciology, 29: 3—19.

Boulton, G. S., 1974: Processes and patterns of glacial erosion. In: Coates (Ed.), Glacial Geomorphology, State University of New York, 41—87.

Boulton, G. S., 1979: Processes of glacier erosion on different substrata. J. Glaciology, 23: 15—38.

Budd, W. F., P. L. Keage and N. A. Blundy, 1979: Empirical studies of ice sliding. J. Glaciology, 23: 157—170.

Drewry, D. J., 1983: Antarctica: Glaciological and Geophysical Folio. University of Cambridge.

Haeberli, W., 1983: Permafrost-glacier relationships in the Swiss Alps — today and in the past. In: Permafrost: Proceedings of the fourth international conference, National Academy Press, Washington D. C., 415—420.

Hallet, B., 1981: Glacial abrasion and sliding: their dependence on debris concentration in basal ice. Ann. of Glaciology, 2: 23—28.

Lliboutry, L. A., 1979: Local friction laws for glaciers: a critical review and new openings. J. Glaciology, 23: 67—95.

Mesinger, F. and A. Arakawa, 1976: Numerical methods used in atmospheric models, Vol. 1. GARP Publication Ser. No. 17, Geneva, 64 pp.

Metcalf, R. C., 1979: Energy dissipation during subglacial abrasion at Nisqually Glacier, Washington, U. S. A. J. Glaciology, 23: 233—246.

Morgan, V. I. and W. F. Budd, 1975: Radioecho sounding of the Lambert Glacier basin. J. Glaciology, 15: 103—111.

Oerlemans, J., 1982: Glacial cycles and ice-sheet modelling. Climatic Change, 4: 353—374.

Oerlemans, J. and C. J. van der Veen, 1984: Ice sheets and climate. Reidel, Dordrecht, 217 pp.

Paterson, W. S. B., 1981: The physics of glaciers. Second edition, Pergamon, Oxford, 380 pp.

Röthlisberger, H., 1968: Erosive processes which are likely to accentuate or reduce the bottom relief of valley glaciers. IAHS Publ. 79: 87—97.

Röthlisberger, H., 1972: Water pressure in intra- and subglacial channels. J. Glaciology, 11: 177—203.

Sugden, D. E. and B. S. John, 1976: Glaciers and landscape. Edward Arnold, London, 376 pp.

Turcotte, D. L., 1979: Flexure. Advances In Geophysics, 21: 51—86.

Turcotte, D. L. and G. Schubert, 1982: Geodynamics. Applications of continuum physics to geological problems. Wiley, New York, 450 pp.

Vivian, R., 1970: Hydrologie et érosion sous-glaciaires. Revue Géogr. Alp., 58: 241—264.

Walcott, R. I., 1970: Isostatic response to loading of the crust in Canada. Can. J. Earth Sci., 7: 716—727.

Manuscript received 30 Jan. 1985, revised 8 July 1985.

Author's address: J. Oerlemans, Institute of Meteorology and Oceanography
University of Utrecht, Princetonplein 5, Utrecht, The Netherlands